Brillouin Spectroscopy of Normal and Keratoconus Corneas

THEO G. SEILER, PENG SHAO, AMIRA ELTONY, THEO SEILER, AND SEOK-HYUN YUN

• PURPOSE: To investigate the age dependence of Brillouin spectroscopy of the cornea and to compare normal and keratoconus corneas.

• DESIGN: Retrospective case-control study.

• METHODS: STUDY POPULATION: Healthy patients and patients suffering from keratoconus seen at the Institut für Refraktive und Ophthalmo-Chirurgie (IROC) between December 2016 and March 2017. Brillouin frequency shifts of patients of 2 different groups were examined with Brillouin spectroscopy perpendicular to the corneal surface. Group 1 consisted of 47 healthy eyes, whereas Group 2 included 36 eyes with keratoconus of unclear progression. Besides Brillouin examinations, corneal tomographies were acquired so that correlations and comparisons between geometric parameters and Brillouin frequency shifts could be evaluated. MAIN OUTCOME MEASURES: Corneal Brillouin frequency shifts averaged over full corneal thickness.

• RESULTS: A significant correlation between age and central Brillouin frequency shift was identified ($P = .011$) with an increase in Brillouin frequency shift of 4 MHz per decade in normal corneas. Keratoconus corneas have a significantly reduced Brillouin frequency shift at the thinnest point compared to normal corneas (5.7072 ± 0.0214 vs 5.7236 ± 0.0146 GHz, $P < .001$). The Brillouin frequency shift at the point of maximum posterior elevation showed best correlation with geometry-derived keratoconus indices. The receiver operating characteristic curve analysis of Brillouin frequency shift showed substantially worse sensitivity and specificity compared to K_{max} and thinnest pachymetry for keratoconus detection.

• CONCLUSION: Noninvasive Brillouin spectroscopy adds clinical information about the biomechanical state of the cornea perpendicular to the surface. An age-dependent stiffening of the cornea has been found and keratoconus corneas are statistically significantly different from normal corneas, but for precise differentiating of keratoconus stages (including normal corneas) the method is currently neither specific nor sensitive enough. Further development including standardized mapping and establishment of new indices may increase the potential of Brillouin spectroscopy substantially. (Am J Ophthalmol 2019;202:118–125.

BRILLOUIN SPECTROSCOPY, INTRODUCED IN ophthalmology in 1980,[1] has recently been heralded to measure mechanical parameters of the cornea noninvasively.[2] The detailed information on corneal biomechanics might have a significant impact on diagnosis of corneal diseases and the predictability of corneal surgery such as keratotomies, but it may also help to interpret the validity of applanation tonometry.[3]

Brillouin spectroscopy measures the interaction of narrow-banded laser light and phonons in matter. Phonons are wavelets produced by molecular vibrations and occur universally in tissue at room temperature, traveling inside matter with a velocity that is related, among others, to the elastic moduli.[4] During this interaction, a small portion of the laser light experiences a frequency shift (Brillouin frequency shift) that is proportional to the velocity of the interacting phonons and, therefore, to the square root of the elastic modulus. Measuring the Brillouin frequency shift in a cornea gives a noninvasive access to the so-called bulk elastic modulus M of the cornea.[5] However, whether this bulk elastic modulus M gives information about the familiar surface-parallel elastic modulus E (Young's modulus) is not yet decided.[6–8]

Keratoconus (KCN) is a chronic disease of the cornea that most probably goes along with an at least localized weakening of the tissue, which results in localized bulging outward.[9,10] This geometric abnormality is mainly the basis of clinical diagnosis of keratoconus and has been characterized by numerous parameters, such as maximal K-reading, corneal coma, astigmatism, other keratoconus indices, and the maximum posterior elevation.[11–14] In contrast, the clinical diagnosis of keratoconus by means of biomechanical minimally invasive methods, for example with the air-puff analyzers, has yet to be questioned.[15] Brillouin spectroscopy would likely be helpful to establish shape-independent biomechanical information about a cornea and could possibly help to diagnose KCN at an earlier stage.

Accepted for publication Feb 5, 2019.

From the Institut für Refraktive und Ophthalmo-Chirurgie (IROC), Zürich, Switzerland (T.G.S., T.S.); the Wellman Center for Photomedicine - Massachusetts General Hospital, Harvard Medical School, Boston, Massachusetts, USA (T.G.S., P.S., A.E., S.H.Y.); and the Universitätsklinik für Augenheilkunde, Inselspital, Bern, Switzerland (T.G.S.).

Inquiries to Theo G. Seiler, Wellman Center for Photomedicine - Massachusetts General Hospital, Harvard Medical School, 50 Blossom St, Boston, MA 02114, USA; e-mails: theo@seiler.tv; gseiler@mgh.harvard.edu

0002-9394/$36.00
https://doi.org/10.1016/j.ajo.2019.02.010

In this retrospective case-control study, we investigate the Brillouin frequency shift measurements in normal and keratoconus corneas and try to compare and correlate the findings with standard geometric keratoconus indices obtained from Scheimpflug tomography.

PATIENTS AND METHODS

• **PATIENTS:** In this retrospective case-control study, 2 groups of patients were examined: (1) patients with normal eyes, to establish a correlation of age and Brillouin frequency shift (n = 47); and (2) patients with KCN, irrespective of progression (n = 36). The patients were asked not to use contact lenses during the 2 weeks before the examination. The study was performed at the Institut für Refraktive und Ophthalmo-Chirurgie (IROC) in Zürich, Switzerland following approval from the Institutional Review Board of Partners HealthCare, the Partners Human Research Committee (PHRC), and the Institutional Review Board of IROC. Informed consent was obtained from every patient before imaging.

Before the Brillouin measurements, corneal tomographies were generated using a commercial topographer (Vario; Wavelight, Erlangen, Germany) and a commercial Scheimpflug camera (Pentacam HR 70700; Oculus, Wetzlar, Germany), including the determination of the thinnest point, the point of maximum posterior elevation, and keratoconus indices. Besides Brillouin spectroscopy, topography, and tomography, the patients received a standard examination consisting of autorefractometry and autokeratometry (Humphrey Model 599; Zeiss, Jena, Germany), anterior segment optical coherence tomography (SS-1000; Tomey, Nagoya, Japan), manifest refraction using the fogging technique, unaided (UDVA) and best spectacle-corrected visual acuity (BSCVA), applanation tonometry, endothelial cell count (SP-02; Construzione Strumenti Oftalmici, Scandicci Firenze, Italy), and slit-lamp examination.

• **GROUP 1:** For normal corneas, 5 axial scans were taken in the central cornea within a radius of 1 mm from the photopic entrance pupil center. From subjects having both eyes scanned (n = 41), only 1 eye was randomly assigned and included. Excluded from the normal group were eyes with any pathology or surgery of the anterior segment (including glaucoma), minimal corneal thickness of less than 500 μm or more than 600 μm, maximal K-readings of less than 40 diopters (D) and more than 47 D, and an age of less than 18 years.

• **GROUP 2:** For keratoconus patients, 20–40 axial scans were taken at different locations, including the point of maximal curvature, the thinnest point, and the point of maximum posterior elevation. The KCN was classified according to Amsler-Krumeich.[16] Excluded from the KCN groups were eyes with classical pellucid marginal degeneration, previous anterior segment surgery including corneal cross-linking, corneal trauma, glaucoma, aphakia, endothelial cell counts less than 2300 cells/mm^2, corneas with no distinctive maximum posterior elevation point, corneal scars that may interfere with Scheimpflug photography, history of recurrent erosions, patients younger than 18 years, pregnancy and breastfeeding, and neurodermitis. If both eyes of a patient fulfilled the inclusion criteria, 1 eye was randomly assigned and included.

• **BRILLOUIN SPECTROSCOPY:** Data were acquired with a custom-made mobile, clinically viable Brillouin scattering microscopy system representing the prototype of the BOSS (Brillouin optical scanning system; Intelon Optics, Boston, Massachusetts, USA). The light source is a single-frequency tunable laser with its output spectrum locked to a near-infrared wavelength of ~780 nm. The laser light is coupled via a polarization-maintaining single-mode fiber to the human interface, in which polarization optics route the laser beam to the eye and direct backscattered light to a single-mode fiber. The spectrometer employs 2-stage virtually imaged phase array (VIPA) etalons to achieve a free-spectral range of ~16 GHz, a resolution of ~0.3 GHz, and an extinction efficiency of −65 dB. The optical power at the cornea is 3–5 mW, which is several times lower than the maximum permissible exposure level according to American National Standards Institute guidelines. With an electron multiplying charge-coupled device (EMCCD, Andor Technology, Belfast, UK) with an integration time of 0.2 seconds, a shot-noise-limited sensitivity of ~±0.008 GHz in Brillouin frequency shift measurement is achieved. During Brillouin frequency shift measurement, the subjects sit with their chin and forehead resting in the human interface headrest, directing their gaze toward a fixation target. For corneal scans, an operator adjusts the human interface using a manual joystick to locate the focus at a desired location in front of the cornea while monitoring an eye-tracking video camera based on pupil detection. The coordinates of special locations, like thinnest point or point of the maximum posterior elevation, were taken from Scheimpflug imaging. Axial scanning from anterior surface to aqueous humor in the anterior chamber is accomplished automatically by a motorized stage carrying the objective lens and, thus, the light focus. Each axial scan comprises 40 points separated by a step size of 35 μm. The EMCCD exposure time for each step is typically 300 ms, resulting in a total axial scan time of about 12 seconds. Data points of 1 axial scan were averaged, resulting in 1 data point in the corresponding x-y position with respect to the pupil center. Reconstructed Brillouin frequency shift maps consisted of at least 40 averaged axial scans using linear interpolation with a step size of 0.1 mm. Axial scanning was carried out with a transverse resolution

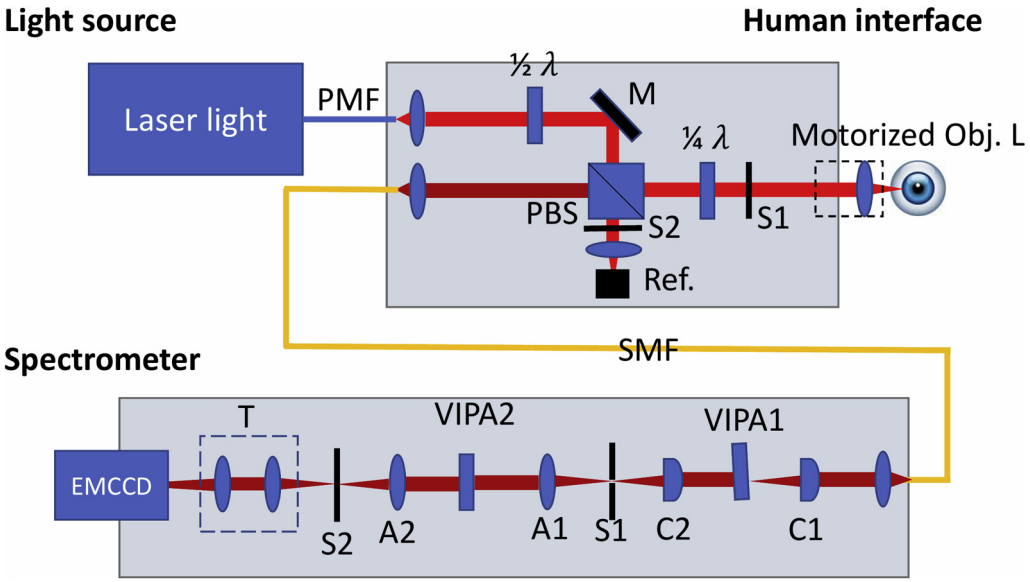

FIGURE 1. Schematic of the Brillouin system. The system is composed of 3 parts: a light source, a human scanning interface built on a modified slit-lamp platform, and a 2-stage virtually imaged phase array (VIPA) spectrometer using 2 crossed-axis VIPA etalons. Human interface: M = mirror; Obj. L = objective lens; PBS = polarizing beam-splitter; PMF = polarization maintaining single-mode fiber; Ref = reference materials; S1/S2 = optical shutters; SMF = single mode fiber; λ/2 = half waveplate; λ/4 = quarter-waveplate. Spectrometer: A1/A2 = achromatic lens; C1/C2 = cylindrical lens; EMCCD = electron multiplying charge-coupled device; S1/S2 = shutters; V1/V2 = VIPAs.

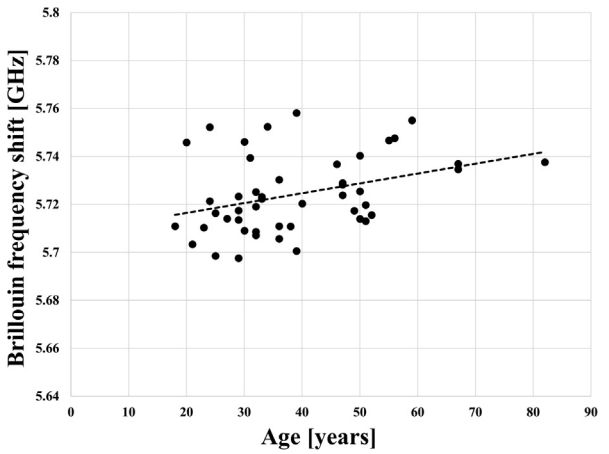

FIGURE 2. Brillouin frequency shifts of healthy corneas from patients aged between 18 and 82 years illustrating a significant correlation ($P = .011$). Linear regression reveals an increase in Brillouin frequency shift of 4 MHz per decade.

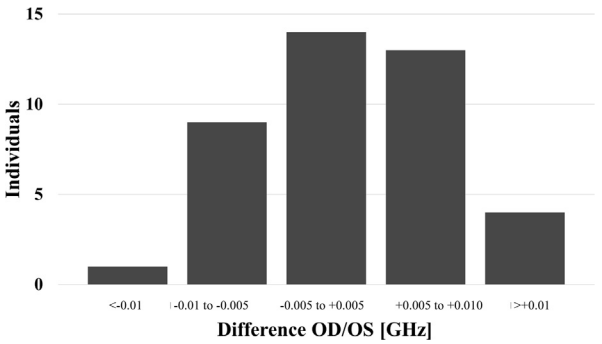

FIGURE 3. Difference in Brillouin frequency shifts between right and left eyes in healthy subjects showing a Gaussian-like distribution.

of ~5 μm. The average total measurement time per eye was less than 15 minutes. The schematic setup is illustrated in Figure 1.

In 3 healthy and 3 keratoconus subjects the intraindividual repeatability of the Brillouin frequency shift was measured to ±0.01 GHz (range, 5 measurements, central measurement corresponding to the x-y position of the entrance pupil center), close to the theoretical limit of ~±0.008 GHz.

• **NUMERICAL ANALYSIS:** Brillouin shifts were reported as average ± standard deviation; demographic parameters were presented as average and range. The correlation of central Brillouin frequency shift and age in the normal group as well as keratoconus parameters in the keratoconus group was established by means of the Spearman rank correlation and 2-sided significance testing using SPSS (IBM, Armonk, New York, USA). The Bonferroni correction was used to avoid accidental significances. The comparison of

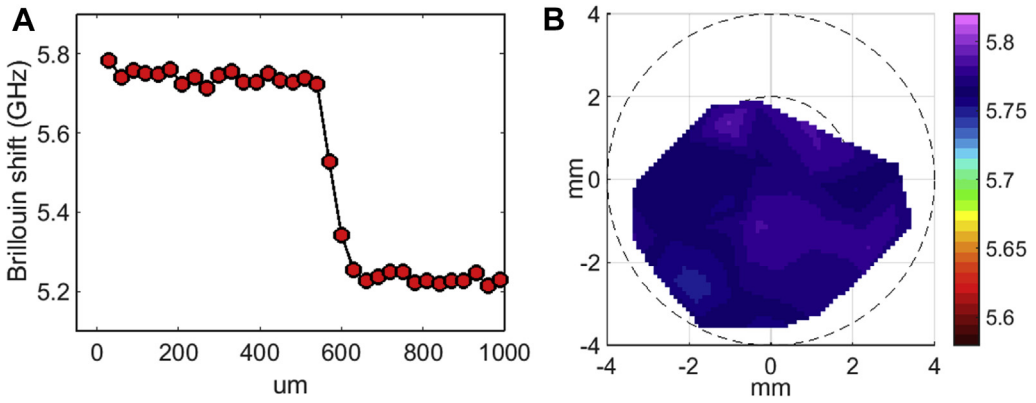

FIGURE 4. (A) A representative axial (depth) scan profile of measured frequency shifts across the cornea and anterior chamber of a healthy subject. (B) A typical Brillouin frequency shift map of a healthy cornea.

TABLE. Correlations and Their Significances of Keratoconus Parameters and Brillouin Frequency Shifts

	B_{thin} (GHz)	B_{MPE} (GHz)
K_{max} (D)	r = −0.20 (*P* = .272)	r = −0.43 (*P* = .039)*
Minimal corneal thickness (μm)	r = 0.34 (*P* = .056)	r = 0.53 (*P* = .010)*
Keratoconus index	r = −0.11 (*P* = .566)	r = −0.48 (*P* = .020)*
Amsler-Krumeich stage	r = −0.16 (*P* = .399)	r = −0.47 (*P* = .023)*

B_{MPE} = Brillouin frequency shift at the point of maximum posterior elevation; B_{thin} = Brillouin frequency shift at the thinnest point of the cornea; D = diopters; K_{max} = maximal keratometry.

Asterisk (*) indicates statistical significance (*P* < .05).

parameters in different groups was performed by means of the Mann-Whitney *U* test. Receiver operating characteristic (ROC) curves were accepted to determine the predictive accuracy of corneal parameters (maximal keratometry [K_{max}], thinnest pachymetry) and Brillouin frequency shift at the point of maximum posterior elevation. These curves are obtained by plotting sensitivity vs 1 − specificity. Except for the correlation testing, all calculations were performed with WinSTAT for Excel (2015; R. Finch Software). Statistical significance was accepted if *P* < .05.

RESULTS

• **GROUP 1: CENTRAL BRILLOUIN FREQUENCY SHIFT IN NORMAL CORNEAS:** The age of subjects included ranged from 18 to 82 years with an average of 39.0 years and a sex distribution of 22:25 (female:male). The central Brillouin frequency shift ($B_{central}$) ranged from 5.6977 to 5.7582 GHz with an average of 5.7242 ± 0.0160 GHz. Age and $B_{central}$ were correlated with a correlation coefficient of 0.369 and a 2-sided *P* value of .011, which declares a statistical significance (Figure 2). Regression analysis using linear, polynomial, and exponential fits yielded the highest regression coefficient R = 0.355 for the linear approach. The slope of the linear regression line is 0.0041 GHz per decade equivalent to 0.07% per decade.

In healthy subjects having both eyes scanned (n = 41), the mean Brillouin frequency shifts were nearly identical for right and left eye: 5.7252 ± 0.0167 GHz vs 5.7222 ± 0.0159 GHz within the instrument's resolution (≤0.01 GHz). The difference between the left and right eyes of each individual subject is a narrowly Gaussian-like distribution (Figure 3) with an average difference of 0.0030 GHz. The bilateral symmetry between the 2 eyes of healthy subjects is remarkable, totally in contrast to the large interpersonal variability.

Within each axial scan a subtle gradient in Brillouin frequency shift was observed, higher in the anterior stroma and decreasing toward the posterior stroma (Figure 4A). A representative axial scan as well as a central reconstructed map of multiple averaged axial scans are depicted in Figure 4.

• **GROUP 2: BRILLOUIN FREQUENCY SHIFT IN KERATOCONUS CORNEAS:** Thirty-six eyes of 36 patients were included in the study. The age ranged from 18 to 63 years with an average of 35.3 years and a sex distribution of 12:24 (female:male). After the normal group was matched

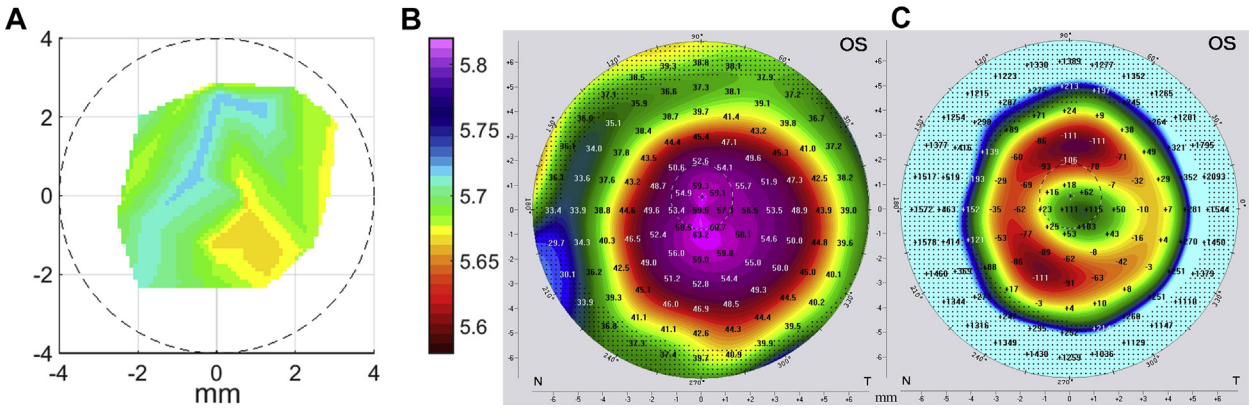

FIGURE 5. A representative keratoconus map (A) is depicted with the corresponding axial curvature (B) and posterior elevation (C, 8-mm best-fit sphere). The Brillouin frequency shift map is centered on the photopic entrance pupil. Curvature and posterior elevation maps are centered on the corneal apex. The pupil is illustrated by the dashed circle, the cross is representing the center of the pupil.

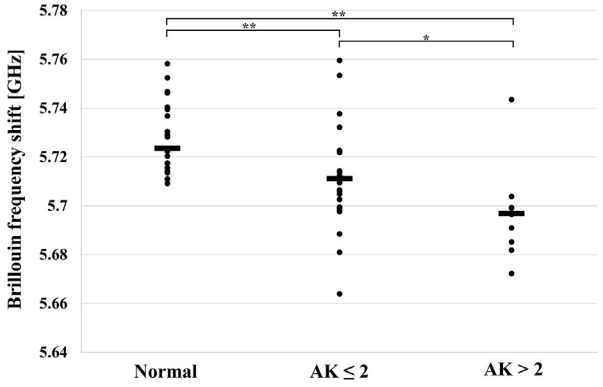

FIGURE 6. Brillouin frequency shifts at the point of thinnest pachymetry in normal corneas and the point of maximum posterior elevation in keratoconus corneas. Keratoconus corneas were subdivided into 2 groups by the Amsler-Krumeich (AK) classification: first group, AK stage 1 and 2; second group, AK stage 3 and 4 (- indicating the average, * indicating significance $P < .05$, ** indicating high significance $P < .01$). It may be of interest that the outlier in the AK > 2 group had a central keratoconus.

to the keratoconus group regarding sex (12:24 vs 12:24) and age (35.4 ± 9.2 years vs 35.3 ± 11.4 years), the $B_{central}$ = 5.7236 ± 0.0146 GHz, which is equivalent to the thinnest point in normal corneas (within the measurement error), could be compared with the Brillouin frequency shift at the thinnest point (B_{thin}) = 5.7072 ± 0.0214 GHz of keratoconus corneas. The difference is highly statistically significant ($P < .001$). Correlation coefficients and their significances between Brillouin frequency shifts at the points of minimal thickness (B_{thin}) or at the maximum posterior elevation (B_{MPE}) and keratoconus parameters (keratoconus index [KI], minimal corneal thickness, K_{max}, Amsler-Krumeich stages) are listed in the Table. This indicates that the bulk modulus at the maximum posterior elevation is better related to specific keratoconus parameters compared to the bulk modulus at the thinnest point. No correlation was found with age, with B_{thin} ($P = .410$), or with B_{MPE} ($P = .682$). In Figure 5, a representative keratoconus Brillouin map with corresponding axial curvature map and posterior elevation map is illustrated.

Subclassification according to Amsler-Krumeich within the keratoconus group resulted in average Brillouin frequency shifts at the point of maximum posterior elevation of 5.7113 ± 0.0210 GHz for stage 1 and 2 and 5.6970 ± 0.0190 GHz for stage 3 and 4. Compared to the matched healthy group, these shifts differ significantly ($P = .009$ for stage 1 and 2 vs $P < .001$ for stage 3 and 4). Between both keratoconus groups a significant difference was observed ($P = .016$). This is illustrated in Figure 6.

The ROC curves of K_{max}, thinnest pachymetry, and Brillouin frequency shift are depicted in Figure 7. The Brillouin frequency shift curve shows a reduced potential to detect keratoconus compared to K_{max} and thinnest pachymetry.

DISCUSSION

THE MAIN FINDINGS OF THIS STUDY ARE AS FOLLOWS: (1) the Brillouin frequency shift (and consequently the bulk modulus) of normal corneas increases with age, with an average rate of approximately 4 MHz per decade; (2) ectatic areas of keratoconus corneas have a highly significantly smaller Brillouin frequency shift than central normal corneas; and (3) at the point of maximum posterior elevation, Brillouin frequency shift correlates significantly with geometric keratoconus indices.

The stiffness of the human cornea increasing with age reflects our daily experience as corneal surgeons: younger

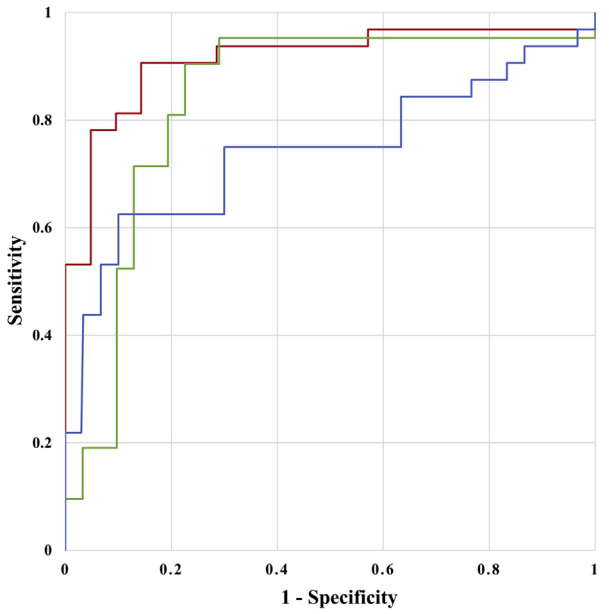

FIGURE 7. Comparison of receiver operating characteristic curves of the single parameters K_{max} (green line), thinnest pachymetry (red line), and Brillouin frequency shift (blue line). The Brillouin frequency shift curve shows a reduced potential to detect keratoconus compared to maximal keratometry and thinnest pachymetry.

corneas are softer compared to corneas of elderly patients. For a century it has been known that ocular rigidity increases with age.[17,18] Aging of living connective tissue generally goes along with increased stiffness (or decreased elasticity), and this effect has been seen in sclera,[19] tendon,[20] skin,[21] and cornea.[22] Elsheikh and associates found a substantial increase of the tangential elastic modulus in 80-year-old corneas compared to 40-year-old corneas,[23] corresponding to an increase of approximately 15% per decade. The age-related increase Brillouin frequency shift measured here was 0.07% per decade, which is at least 2 orders of magnitude less compared to surface-parallel elastic modulus. Does the Brillouin frequency shift reflect biomechanical parameters that are different from the familiar biomechanical transverse moduli measured by extensiometry? Reiss and associates state that neither Young's elastic modulus (E) nor the shear modulus (G) can be determined from measurements of the surface-perpendicular Brillouin frequency shift.[6] Also, Lepert and associates believe that at the current state of knowledge it is not appropriate to convert the measured Brillouin frequency shifts into mechanical moduli.[7] In contrast, Scarcelli and associates claim that the bulk modulus determined from the Brillouin frequency shift in the cornea is related to conventional Young's (or shear) moduli through a log-log linear relationship[24]; however, this was shown only for the surface-perpendicular compression modulus in porcine crystalline lens nuclei.[5] The lens nucleus may be considered an isotropic matter, and to transfer this technique to cornea may not be correct because the cornea is highly anisotropic. The lamellar ultrastructure of the cornea demands different elastic moduli regarding surface-parallel in contrast to surface-perpendicular measurements. Recently, we were able to show that the Brillouin frequency shift (and, therefore, the bulk modulus) of the rabbit cornea is independent of surface-parallel stress up to an intraocular pressure of 75 mm Hg.[8] To prevent misinterpretations, we report here about Brillouin frequency shift rather than about Brillouin bulk modulus.

Kohlhaas and associates found a 2.7-fold increase between the anterior half of human corneas compared to the posterior half using tangential extensiometry.[25] Also, Brillouin spectroscopy finds a higher value in the anterior stroma compared to posterior stroma, albeit only with a minor difference. Again, Brillouin spectroscopy is measuring the surface-perpendicular bulk modulus, which should not be confused with the surface-parallel elastic modulus.

The difference in Brillouin frequency shift between fellow eyes was tested in 41 patients. The average difference was comparable to the measurement error of the device and is therefore negligible. This is in substantial contrast to the much higher interindividual variability (Figure 2) and may indicate that the bulk modulus represents a personal parameter, characterizing both eyes simultaneously in heathy individuals.

Scarcelli and associates found in ex vivo experiments that keratoconus corneas show a smaller bulk modulus compared to normal corneas.[26] In the present study the difference between normal and KCN corneas is highly significant; however, the absolute difference of the Brillouin frequency shifts is only in the order of the standard deviation of the 2 groups. Therefore, 1 single measurement of Brillouin frequency shift is neither specific nor sensitive enough to allow a diagnostic discrimination between KCN and normal cornea. This is underlined by the ROC curves that demonstrate the weaker potential of Brillouin frequency shift compared to K_{max} and thinnest pachymetry. On the other hand, a parameter like thickness or curvature in 1 single point alone is generally not a good measure, and it is the overall geometric distribution of values that defines diagnosis. The next generation of clinical Brillouin spectrometers will have a scanner and eye-tracker system to facilitate reproducible Brillouin maps of the cornea. As mentioned before, the current Brillouin spectrometers employ the measurements in a surface-perpendicular direction; however, the clinically relevant elastic modulus is determined in a surface-parallel plane. Therefore, the measurement direction of a clinically useful Brillouin spectrometer will have to be also surface-parallel.

Another approach to measure ocular biomechanics is the air puff–induced deformation of the corneal shape. Although sclera, intraocular pressure, and other extraocular tissues are contributing to the deformation behavior of the cornea,[27] parameters were determined that allow an

assessment of corneal biomechanics in vivo. Recently, Vinciguerra and others were able to distinguish keratoconus corneas from healthy corneas using the Corvis ST device[28, 29] with a sensitivity of 94.1% and a specificity of 100%. Whereas the deformation-based analysis of the cornea does not yield spatially resolved data, Brillouin spectroscopy offers the spatial resolution at different points of the cornea. On the other hand, the current technique of Brillouin spectroscopy is not capable of separating early keratoconus corneas from normal corneas by 1 measurement value because of a significant overlap (Figure 6).

Clinically accepted keratoconus parameters like minimal thickness or K_{max} correlate with the Brillouin frequency shift, and the most significant correlation was obtained for Brillouin frequency shifts measured over the area around the maximum posterior elevation. Brillouin frequency shifts at the point of minimal thickness or, even worse, the point of K_{max} correlated much more weakly, indicating that near the point of maximum posterior elevation the cornea is softest. This is supported by the fact that in keratoconus the epithelium thickness modulates corneal thickness as well as anterior curvature.[30] The epithelium is thinner in the center of the ectasia and thicker around the ectasia, with the potential of masking the stromal point bulging forward. Since corneal endothelium consists of a single layer of cells,[31] the posterior surface measured by optical coherence tomography (and, less reliably, with Scheimpflug photography) indicates the locus of maximal protrusion and consequently the weakest area of the cornea at best.

Besides the limitation arising from surface-perpendicular instead of surface-parallel measurements, there are other limitations that need to be addressed: (1) the tomographic shape of the cornea needs to be known prior to Brillouin spectroscopy in order to find the thinnest point or the point of maximum posterior elevation; (2) the total measurement time of 15 minutes per cornea is too long for a clinical routine; (3) the measurement location on the cornea needs to be captured, which requires an active eye tracker; and (4) the spectral frequency resolution of 0.008 GHz is too high compared to the total measurement range of the 0.1 GHz, because this implies only 12 categories of Brillouin frequency shift. In addition, only corneas with a distinctive maximum in posterior elevation were included, which might act a potential bias.

In summary, the noninvasive measurement of the Brillouin frequency shift in the cornea adds clinical information about the surface-perpendicular biomechanical state of a cornea. Although the response of keratoconus corneas is statistically different from that of normal corneas, a differential diagnosis is currently not possible because of the lack of specificity and sensitivity.

FUNDING/SUPPORT: THE PROJECT WAS FUNDED BY THE U.S. NATIONAL INSTITUTES OF HEALTH (R01EY025454, P41EB015903) AND the Harvard Catalyst Incubator program (UL1-RR025758). Financial Disclosures: Peng Shao, Theo Seiler, and Seok-Hyun Yun are scientific consultants of Intelon Inc, Boston, Massachusetts, USA. Theo Seiler is also a scientific consultant of Avedro Inc, Waltham, Massachusetts, USA. The following authors have no financial disclosures: Theo G. Seiler and Amira Eltony. Drs Seiler and Shao served jointly as first authors. All authors attest that they meet the current ICMJE criteria for authorship.

REFERENCES

1. Vaughan JM, Randall JT. Brillouin scattering, density and elastic properties of the lens and cornea of the eye. *Nature* 1980;284:489–491.
2. Scarcelli G, Pineda R, Yun SH. Brillouin optical microscopy for corneal biomechanics. *Invest Ophthalmol Vis Sci* 2012;53:185–190.
3. Liu J, Roberts CJ. Influence of corneal biomechanical properties on intraocular pressure measurement: quantitative analysis. *J Cataract Refract Surg* 2005;31:146–155.
4. Brillouin L. Diffusion de la lumière et des rayons X par un corps transparent homogène - Influence de l'agitation thermique. *Ann Phys* 1922;9:88–122.
5. Scarcelli G, Kim P, Yun SH. In vivo measurement of age-related stiffening in the crystalline lens by Brillouin optical microscopy. *Biophys J* 2011;101:1539–1545.
6. Reiß S, Burau G, Stachs O, et al. Spatially resolved Brillouin spectroscopy to determine the rheological properties of the eye lens. *Biomed Opt Express* 2011;2:2144–2159.
7. Lepert G, Gouveia RM, Connon CJ, Paterson C. Assessing corneal biomechanics with Brillouin spectro-microscopy. *Faraday Discuss* 2016;187:415–428.
8. Seiler TG, Shao P, Frueh BE, Yun SH, Seiler T. The influence of hydration on different mechanical moduli of the cornea. *Graefes Arch Clin Exp Ophthalmol* 2018;256:1653–1660.
9. Horner JF. Zur Behandlung des Keratoconus. *Klin Monbl Augenheilkd* 1869;5:24–26.
10. Andreassen TT, Simonsen AH, Oxlund H. Biomechanical properties of keratoconus and normal corneas. *Exp Eye Res* 1980;31:435–441.
11. Belin MW, Ambrósio R. Scheimpflug imaging for keratoconus and ectatic disease. *Indian J Ophthalmol* 2013;61:401–406.
12. Maeda N, Klyce SD, Smolek MK. Comparison of methods for detecting keratoconus using videokeratography. *Arch Ophthalmol* 1995;113:870–874.
13. Rabinowitz YS. Videokeratographic indices to aid in screening for keratoconus. *J Refract Surg* 1995;11:371–379.
14. Randleman JB, Dupps WJ Jr, Santhiago MR, et al. Screening for keratoconus and related ectatic corneal disorders. *Cornea* 2015;34:e20–e22.
15. Vellara HR, Patel DV. Biomechanical properties of the keratoconic cornea: a review. *Clin Exp Optom* 2015;98:31–38.
16. Amsler M. Kératocõne classique et kératocône fruste; arguments unitaires. *Ophthalmologica* 1946;111:96–101.
17. Friedenwald JS. Contribution to the theory and practice of tonometry. *Am J Ophthalmol* 1937;20:985–1024.

18. Pallikaris IG, Kymionis GD, Ginis HS, Kounis GA, Tsilimbaris MK. Ocular rigidity in living human eyes. *Invest Ophthalmol Vis Sci* 2005;46:409–414.
19. Friberg TR, Lace JW. A comparison of the elastic properties of human choroid and sclera. *Exp Eye Res* 1988;47:429–436.
20. Gillis C, Pool RR, Meagher DM, Stover SM, Reiser K, Willits N. Effect of maturation and aging on the histomorphometric and biochemical characteristics of equine superficial digital flexor tendon. *Am J Vet Res* 1997;58:425–430.
21. Biniek K, Kaczvinsky J, Matts P, Dauskardt RH. Understanding age-induced alterations to the biomechanical barrier function of human stratum corneum. *J Dermatol Sci* 2015;80:94–101.
22. Malik NS, Moss SJ, Ahmed N, Furth AJ, Wall RS, Meek KM. Ageing of the human corneal stroma: structural and biochemical changes. *Biochim Biophys Acta* 1992;1138:222–228.
23. Elsheikh A, Geraghty B, Rama P, Campanelli M, Meek KM. Characterization of age-related variation in corneal biomechanical properties. *J R Soc Interface* 2010;7:1475–1485.
24. Scarcelli G, Kling S, Quijano E, Pineda R, Marcos S, Yun SH. Brillouin microscopy of collagen crosslinking: noncontact depth-dependent analysis of corneal elastic modulus. *Invest Ophthalmol Vis Sci* 2013;54:1418–1425.
25. Kohlhaas M, Spoerl E, Schilde T, Unger G, Wittig C, Pillunat LE. Biomechanical evidence of the distribution of cross-links in corneas treated with riboflavin and ultraviolet A light. *J Cataract Refract Surg* 2006;32:279–283.
26. Scarcelli G, Besner S, Pineda R, Yun SH. Biomechanical characterization of keratoconus corneas ex vivo with Brillouin microscopy. *Invest Ophthalmol Vis Sci* 2014;55:4490–4495.
27. Kling S, Marcos S. Contributing factors to corneal deformation in air puff measurements. *Invest Ophthalmol Vis Sci* 2013;54:5078–5085.
28. Vinciguerra R, Ambrósio R Jr, Elsheikh A, et al. Detection of keratoconus with a new biomechanical index. *J Refract Surg* 2016;32:803–810.
29. Wang YM, Chan TCY, Yu M, Jhanji V. Comparison of corneal dynamic and tomographic analysis in normal, forme fruste keratoconic, and keratoconic eyes. *J Refract Surg* 2017;33:632–638.
30. Reinstein DZ, Archer TJ, Gobbe M. Corneal epithelial thickness profile in the diagnosis of keratoconus. *J Refract Surg* 2009;25:604–610.
31. Maurice DM. The cornea and the sclera. In: In: Davson H, ed. The Eye. 3rd ed., Vol 1b. Orlando, FL: Academic Press; 1984:1–158.